Supporting Information

for

Smart hybridization of $Sn_2Nb_2O_7/SnO_2$@3D carbon nanocomposites with enhanced sodium storage performance through self-buffering effects

Pengbo Zhai,[a] Jian Qin,[a] Lichao Guo,[a] Naiqin Zhao,[ab] Chunsheng Shi,[a] En-Zuo Liu,[ab] Fang He,[a] Liying Ma,[a] Jiajun Li[a] and Chunnian He*[ab]

[a] *School of Materials Science and Engineering and Tianjin Key Laboratory of Composites and Functional Materials, Tianjin University, Tianjin 300072, China.*

**E-mail: cnhe08@tju.edu.cn*

[b] *Collaborative Innovation Center of Chemical Science and Engineering, Tianjin 300072, China*

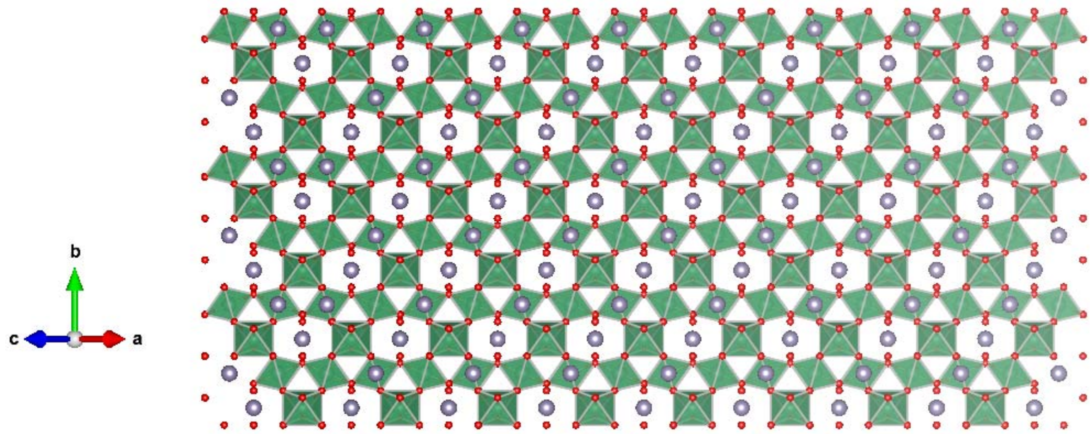

Fig. S1 Typical crystal structure of $Sn_2Nb_2O_7$ looking from the crystal direction of [101].

From Fig S1, we can clearly observe the arrangement of Sn, Nb, O atoms. The Sn atoms are surrounded by the green NbO_6 octahedra while the Nb and Sn distribute uniformly in the whole crystal. [S1] After the first discharge process, the crystal structure becomes amorphous because of the insertion of Na^+ but the Sn, Nb and O will still maintain a uniform distribution.

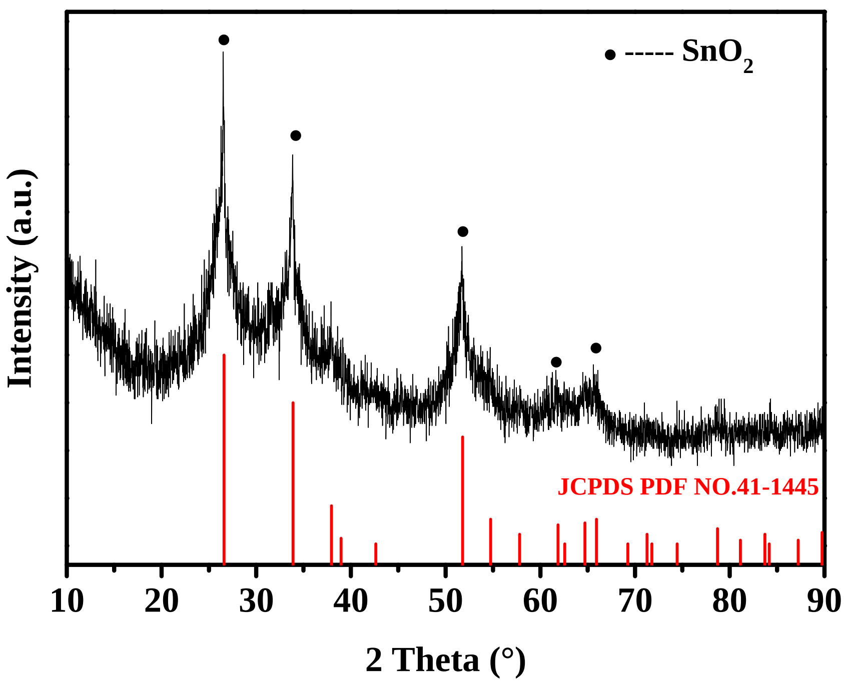

Fig. S2 XRD pattern of SnO_2/3DC

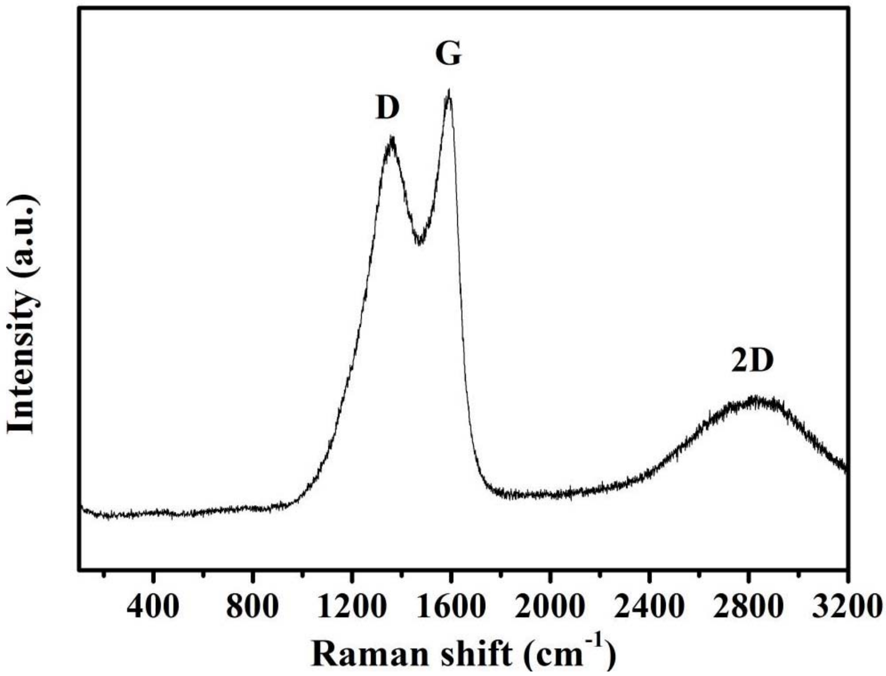

Fig. S3 Raman spectrum of $SnO_2/Sn_2Nb_2O_7$@3DC hybrids.

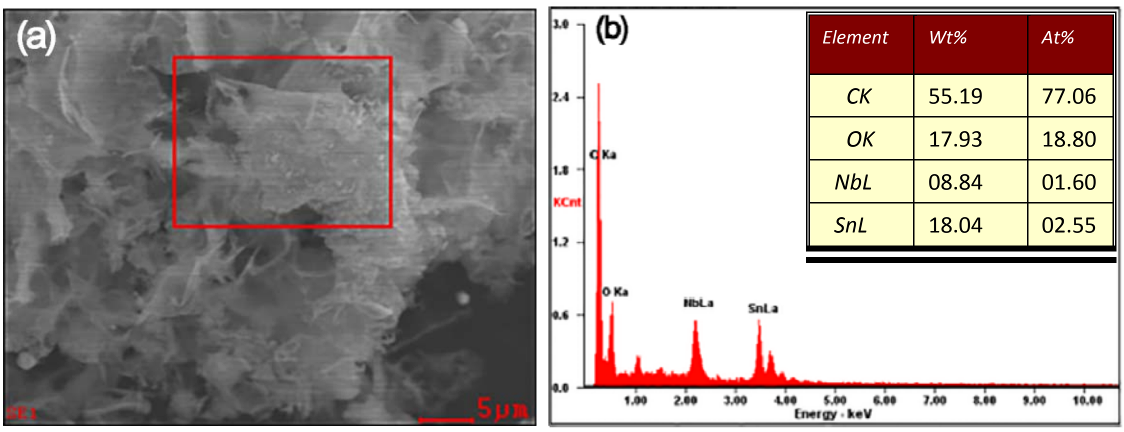

Fig. S4 (a) Low-magnified SEM image of as-synthesized $SnO_2/Sn_2Nb_2O_7$@3DC; (b) EDX spectrum of red wire frame area in (a).

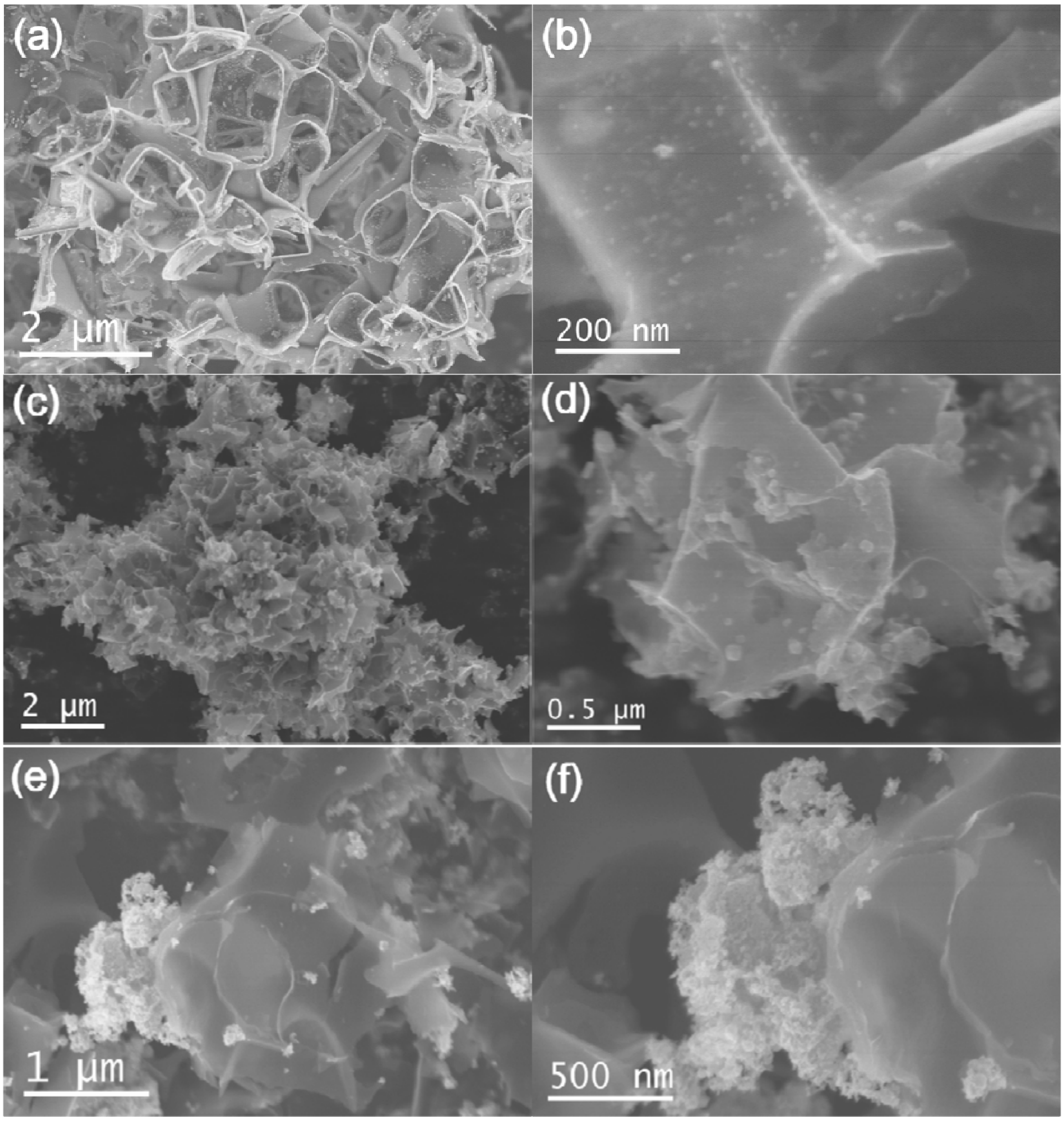

Fig. S5 Typical SEM images of (a, b) SnO_2/3DC; (c, d) Nb_2O_5/3DC and (e, f) SnO_2/Nb_2O_5/3DC.

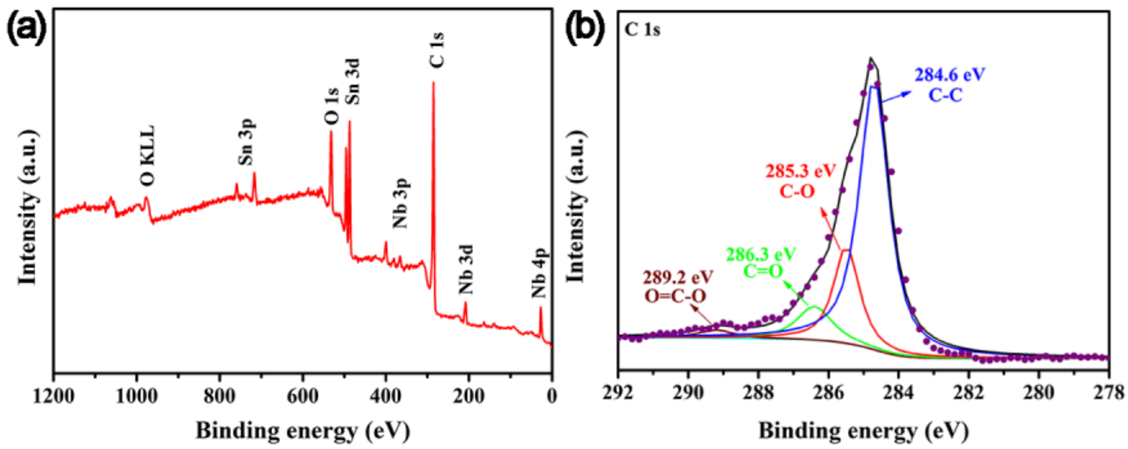

Fig. S6 (a) XPS survey scan of $SnO_2/Sn_2Nb_2O_7$@3DC hybrids; (b) High resolution XPS spectra for C.

From the Fig. S6 (a), we can see that the as-obtained $SnO_2/Sn_2Nb_2O_7$@3DC hybrids only contains the elements of Sn, Nb, C and O. In Fig S6 (b), the binding energy peaks located at 284.6, 285.3, 286.3 and 289.2 eV are corresponding to the C-C, C-O, C=O, and O=C-O bonds, respectively. These bonds between C and O come from the residual oxycarbide groups. [S2]

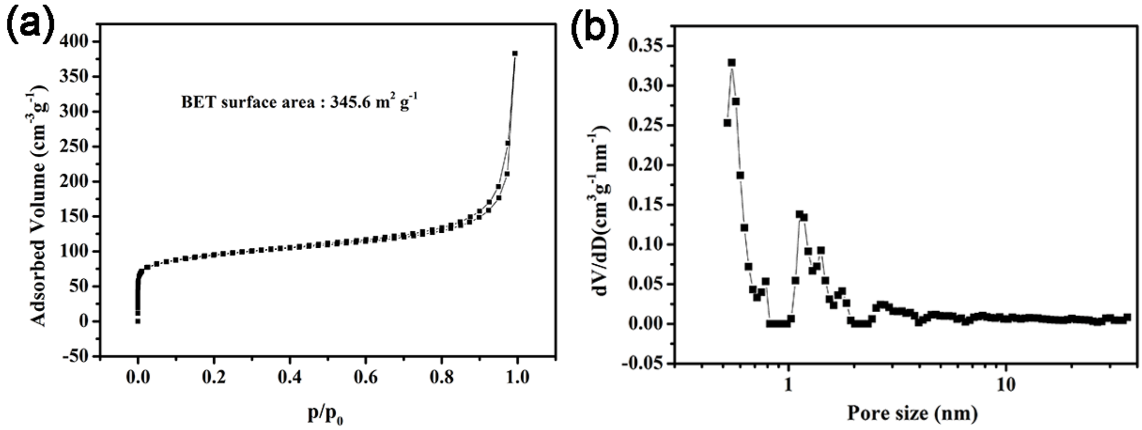

Fig. S7 (a) Nitrogen adsorption-desorption isotherms and (b) DFT pore size distribution curve of $SnO_2/Sn_2Nb_2O_7$@3DC.

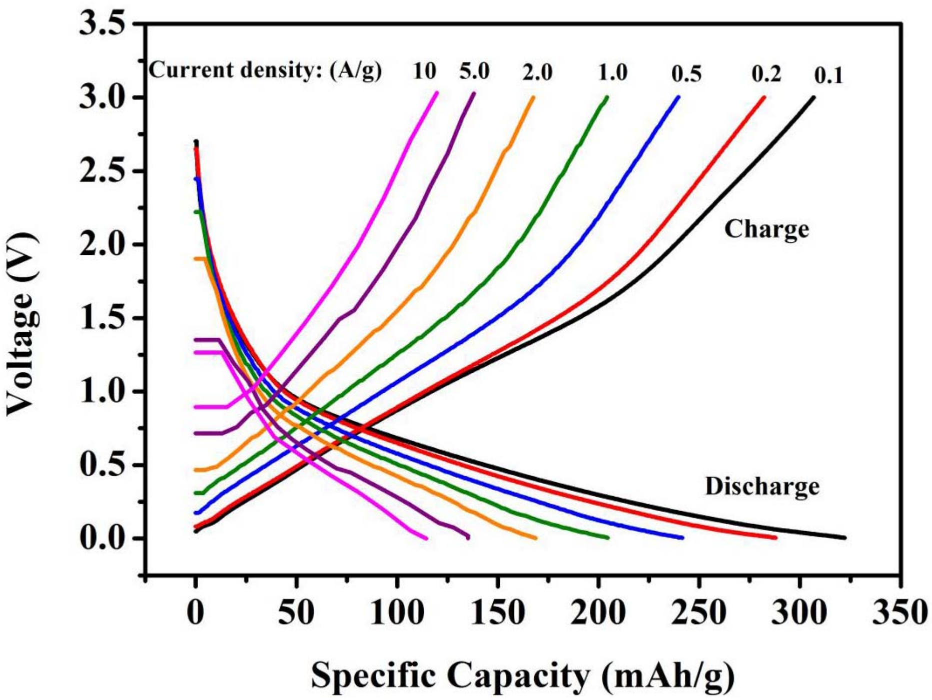

Fig. S8 Galvanostatic discharge/charge profiles of the M-$Sn_2Nb_2O_7/SnO_2$@3DC electrode at various current densities of 0.1, 0.2, 0.5, 1.0, 2.0, 5.0, and 10 A g^{-1}.

Table S1 Comparison of specific capacity and capacity retention at different current densities for different cycle numbers for M-$Sn_2Nb_2O_7$/SnO_2@3DC electrode with other simple composites of SnO_2/Carbon and Nb_2O_5/Carbon.

Sample	Current density ($A\ g^{-1}$)	Specific capacity ($mAh\ g^{-1}$)	Cycle number	Capacity retention (%)
M-$Sn_2Nb_2O_7$/SnO_2@3DC (this work)	0.1	295	100	97.7
	5.0	130	5000	96.3
G-Nb_2O_5 nanosheets (ref S3)	0.05	230	30	76.7
	4.0	100	1000	90
SnO_2-PC (ref S4)	0.1	280.1	250	91.6
	1.6	100	1000	93.4
Nb_2O_5@C/rGO-50 (ref S5)	0.125	200	300	80
	1.25	130	500	86.7
Al_2O_3/SnO_2/CC (ref S6)	0.134	375	100	80
Nb_2O_5 NCs/rGO (ref S7)	0.2	181	100	69.2
a-SnO_2/GA (ref S8)	0.05	380.2	100	91.7
m-Nb_2O_5-C (ref S9)	0.05	175	50	94.6
	0.1	100	300	67
SnO_2/GNS-$SCCO_2$ (ref S10)	0.02	280	100	82

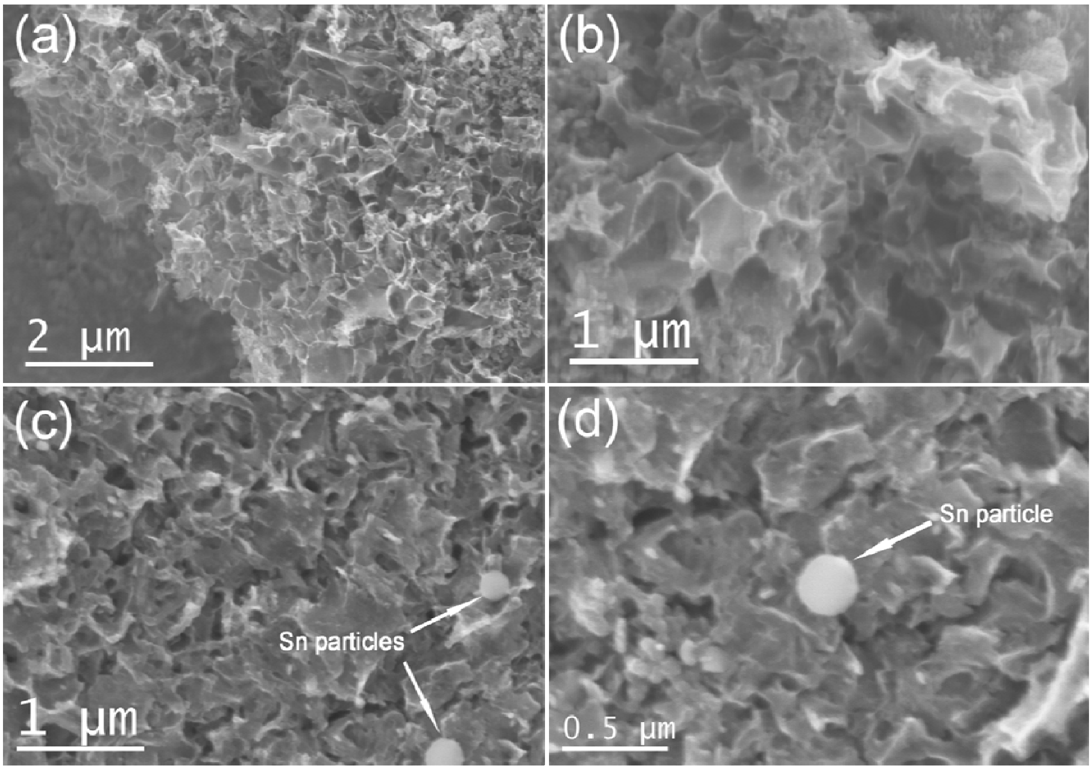

Fig. S9 (a, b) Typical SEM images of a M-$Sn_2Nb_2O_7/SnO_2$@3DC electrode after 100 electrochemical cycles; (c, d) Typical SEM images of a SnO_2/3DC electrode after 100 electrochemical cycles.

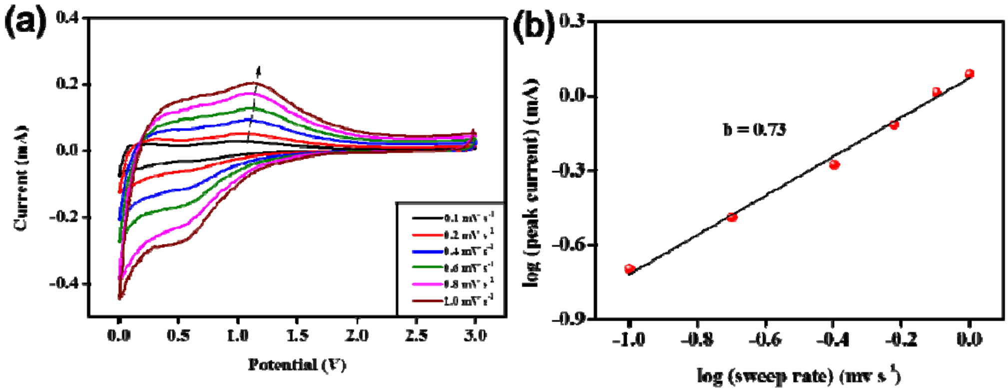

Fig. S10 (a) Cyclic voltammetry curves of SnO_2@3DC electrode at different scan rate ranging from 0.1 to 1.0 mV^{-1}; (b) Plot of log(i) vs log(v) of anodic peaks (red spheres) and corresponding b-value determination (black lines) according to the power law ($i = av^b$). The b value is 0.73 indicating that the electrochemical reactions of SnO_2@3DC electrode is mainly diffusion-controlled.

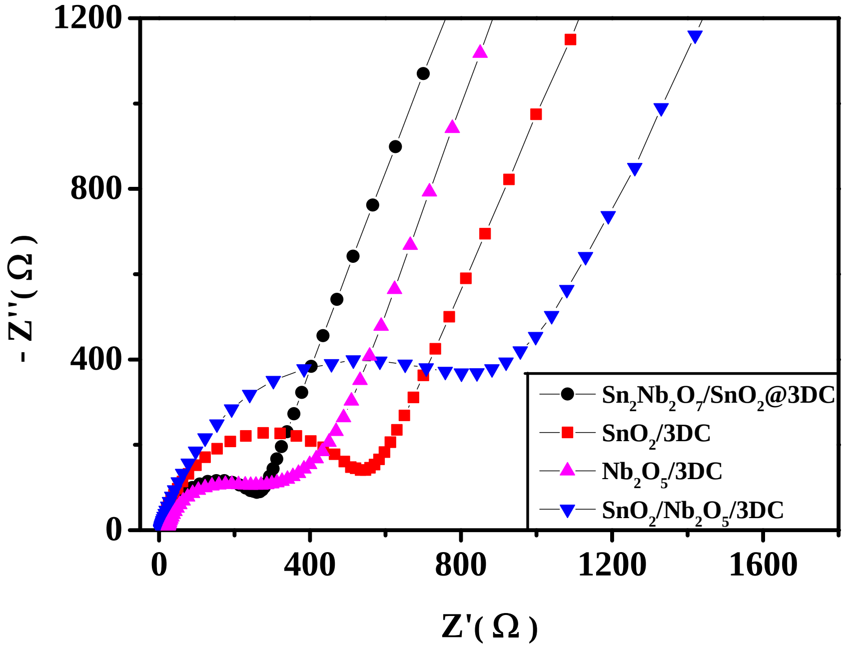

Fig. S11 Nyquist plots of M-$Sn_2Nb_2O_7/SnO_2$@3DC, SnO_2@3DC, Nb_2O_5/3DC and mechanical mixing of SnO_2/Nb_2O_5/3DC electrodes after the rate tests over the frequency range from 100 kHz to 10 mHz.

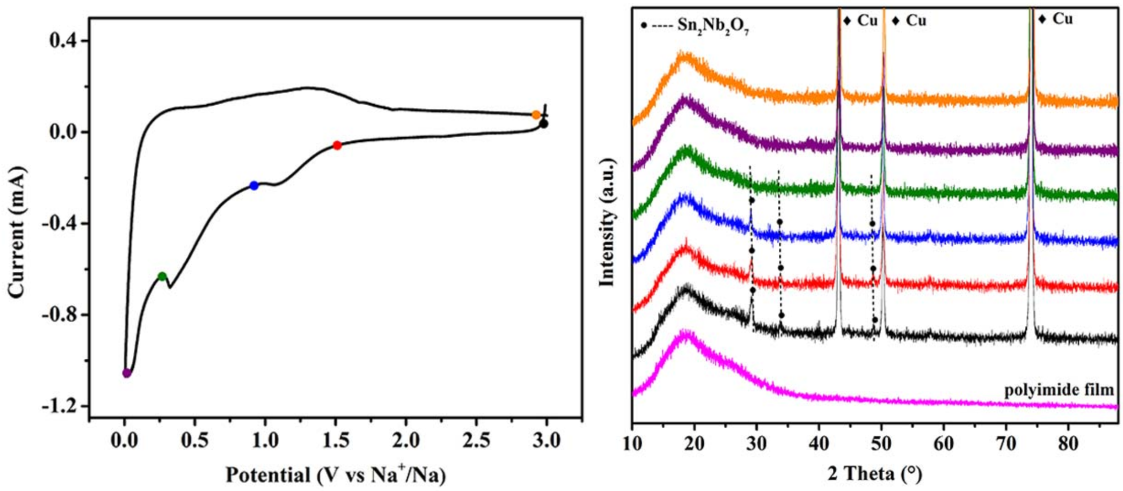

Fig. S12 Ex-situ XRD patterns obtained at different state of the first discharge-charge process to understand the structural change of M-$Sn_2Nb_2O_7$/SnO_2@3DC electrode

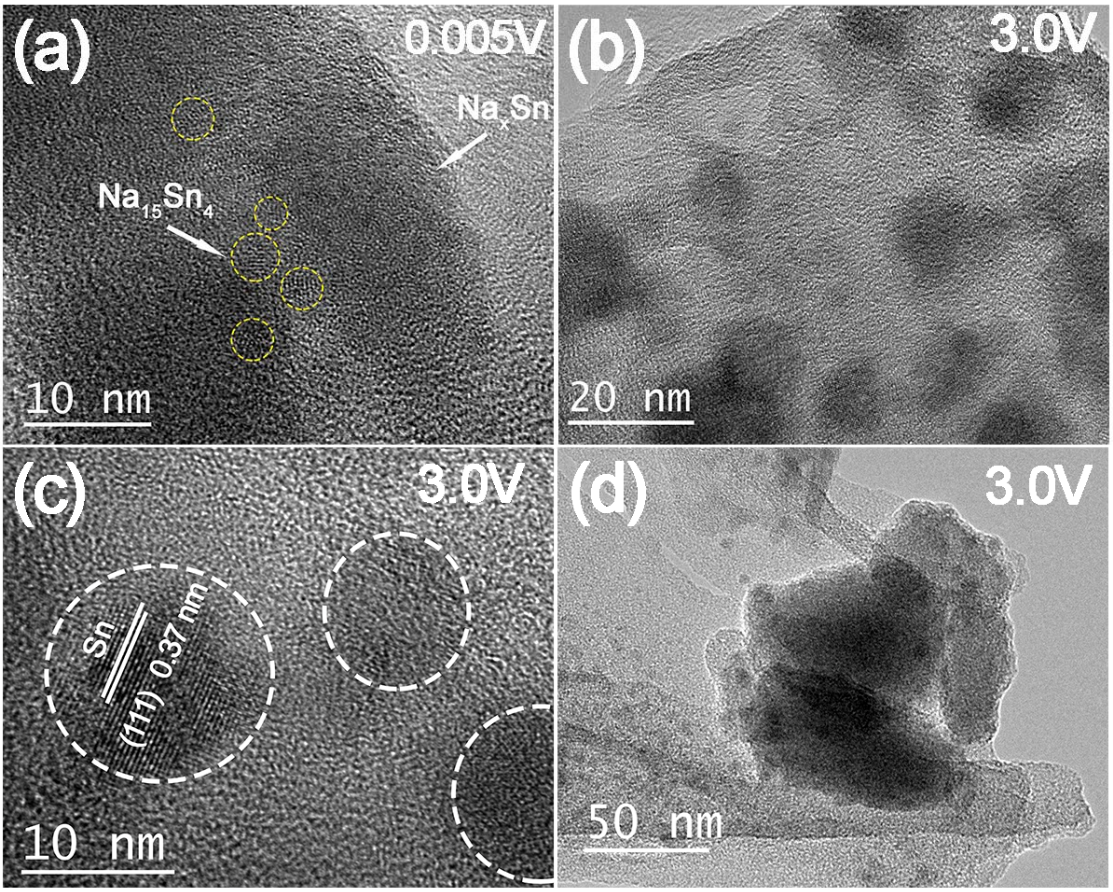

Fig. S13 (a) HRTEM image of M-$Sn_2Nb_2O_7$/SnO_2@3DC electrode material obtained at the discharged voltage of 0.005V; (b, c) charged voltage of 3.0V and (d) TEM image at the charged voltage of 3.0V.

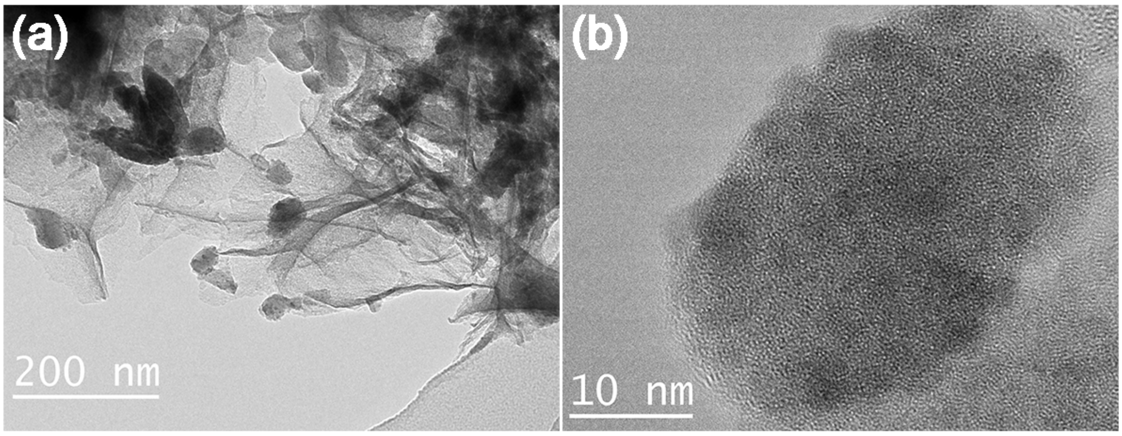

Fig. S14 (a) TEM image and (b) HRTEM image of M-$Sn_2Nb_2O_7$/SnO_2@3DC electrode after rate performance test.

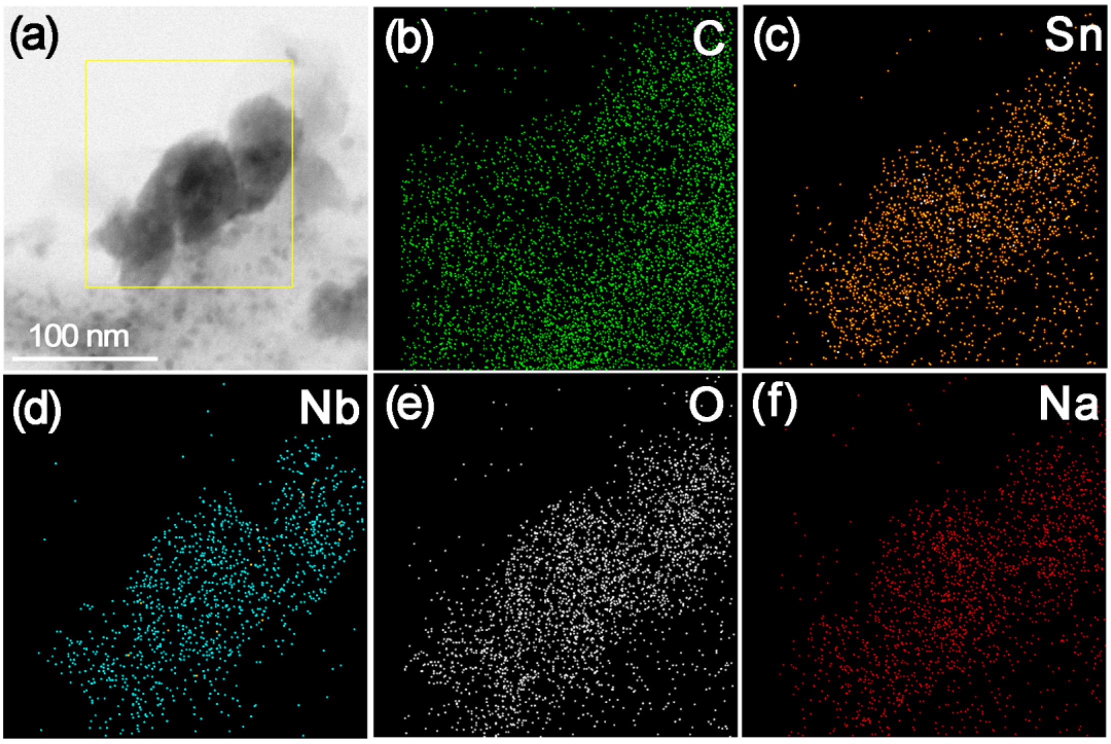

Fig. S15 (a) STEM BF image and the corresponding elemental mapping images of (b) carbon; (c) tin; (d) niobium; (e) oxygen and (f) sodium.

References:

S1. Hosogi, Y.; Shimodaira, Y.; Kato, H.; Kobayashi, H.; Kudo, A., *Chem. Mater.*, 2008, *20* (4), 1299-1307.
S2. Chen, B.; Liu, E.; He, F.; Shi, C.; He, C.; Li, J.; Zhao, N., *Nano Energy,* 2016, *26*, 541-549.
S3. Wang, L.; Bi, X.; Yang, S., *Adv. Mater*, 2016, *28* (35), 7672-9.
S4. Huang, Z.; Hou, H.; Zou, G.; Chen, J.; Zhang, Y.; Liao, H.; Li, S.; Ji, X., *Electrochim Acta* 2016, *214*, 156-164.
S5. Lim, E.; Jo, C.; Kim, M. S.; Kim, M. H.; Chun, J.; Kim, H.; Park, J.; Roh, K. C.; Kang, K.; Yoon, S.; Lee, J., *Adv. Funct. Mater.*, 2016, *26* (21), 3711-3719.
S6. Liu, Y.; Fang, X.; Ge, M.; Rong, J.; Shen, C.; Zhang, A.; Enaya, H. A.; Zhou, C., *Nano energy* 2015, *16*, 399-407.
S7. Yan, L.; Chen, G.; Sarker, S.; Richins, S.; Wang, H.; Xu, W.; Rui, X.; Luo, H., *ACS Appl. Mat. Interfaces,* 2016, *8* (34), 22213-22219.
S8. Fan, L.; Li, X.; Yan, B.; Feng, J.; Xiong, D.; Li, D.; Gu, L.; Wen, Y.; Lawes, S.; Sun, X., *Adv. Energy Mater.*, 2016, *6* (10), 1502057.
S9. Kim, H.; Lim, E.; Jo, C.; Yoon, G.; Hwang, J.; Jeong, S.; Lee, J.; Kang, K., *Nano Energy* 2015, *16*, 62-70.
S10. Patra, J.; Chen, H.-C.; Yang, C.-H.; Hsieh, C.-T.; Su, C.-Y.; Chang, J.-K., *Nano Energy* 2016, *28*, 124-134.